Broadband PureB Ge-on-Si Photodiodes

Lis K. Nanver, *Life Member, IEEE*, Vinayak V. Hassan, *Member, IEEE*, Asma Attariabad, Nicholas Rosson, and Chantal J. Arena

***Abstract*— Broadband PureB Ge-on-Si photodiodes were fabricated by *in-situ* capping of n-type Ge-islands grown by chemical-vapor deposition on Si with a 10-nm-thick pure boron layer. Using deposition temperatures from 575°C - 700°C, the B-layer forms p^+-like anodes with nm-shallow junctions and low dark currents, enabling close to ideal responsivities of 0.13, 0.37, 0.48, and 0.19 A/W at wavelengths 406, 670, 1310 and 1550 nm, respectively.**

***Index Terms*— Broadband, chemical-vapor deposition, germanium, pure boron, photodiodes, responsivity, ultra-shallow junctions.**

I. Introduction

WHILE silicon remains the mainstream microelectronics material, the higher mobility and optical infrared absorption of Ge has positioned it as an important material for integration in both CMOS and Si-based photonic circuits (PICs) [1], [2]. Particularly important in this respect has been the development over the last two decades of methods for growing high-quality Ge crystals directly on Si substrates [3], [4], [5]. For the integration of Ge IR photodiodes, the performance is often limited by high dark currents related to defects and/or poor passivation of the p-n junctions. With respect to responsivity, Ge photodiodes are usually only characterized down to about 600 nm, below which the junction is mainly too deep compared to the absorption length of the light [6], [7], [8].

In silicon, the depth of highly-doped junctions also impeded the fabrication of efficient VUV and low-energy-electron photodiodes. PureB technology was introduced as a potent solution [9], [10], offering nm-shallow p^+-n-like junctions by using low-temperature deposition of down to 2-nm-thick pure boron layers directly on the Si. This damage-free fabrication method also ensured low dark currents, and, of major importance for the application, high stability and robustness were achieved due to the very stable B-Si interface containing a high concentration of fixed negative charge combined with the chemically resilient nature of the B-layer itself [11], [12].

Initial experiments applying B deposited directly on Ge did not result in diodes with low dark currents, which was thought to be due to low the diffusivity/solubility of B in Ge [8]. On Si, a wetting layer of Ga deposited at 400°C was found to also form p^+-like regions [13], and, when capped by a 400°C B-layer, this "PureGaB" diode displayed much better B material properties than PureB-only diodes [14]. On Ge, this motivated the use of a Ga wetting layer to provide damage-free p-doping. A capping layer of B was also applied, functioning as a material barrier to Al metallization [15]. In this way, PureGaB Ge-on-Si photodiodes were fabricated with low dark currents and broadband responsivity verified down to 255 nm [16].

The PureGaB Ge-on-Si results were very promising but the deposition of Ga in the chemical-vapor-deposition (CVD) reactors being used, such as the ASM Epsilon, proved problematic due to the corrosive nature of Ga deposited on the walls of the quartz deposition chambers. Therefore, focus has shifted to the PureB option. In this letter we present work that has resulted in the fabrication of PureB Ge-on-Si photodiodes with low dark currents and high responsivity for wavelengths from 406 nm to 1550 nm.

II. Experimental Procedures

For this study of diodes fabricated by depositing pure B on Ge, 4 wafers with Ge islands grown in the same way were available. A schematic cross section along with images of the fabricated devices are shown in Fig.1. The Si substrates were 2–5 ohm-cm n-type (100) 100-mm wafers covered with 1-μm-thick thermal SiO_2. They were patterned with windows plasma-etched to the Si surface in areas ranging from 4×4 μm^2 to 1×1 cm^2. All the depositions were performed in an ASM Epsilon 2000 CVD reactor equipped with germane (GeH_4) and diborane (B_2H_6) carrier gases. After native oxide removal, Ge islands were grown with high selectively in the oxide windows at 385-425°C and annealed at 850°C for 2 min. The growth was strong in the <100> direction and inhibited in the <311> direction, resulting in flat-top pyramids with no Ge attached to the SiO_2 sidewalls. The Ge flat-top thickness was 1450±5 nm for the 25×25 μm^2 diodes used to measure responsivity.

Without vacuum break, the Ge-islands were capped with a targeted 10-nm-thick B-layer grown with the 4 different pressure/temperature combinations listed in Table I.

Manuscript received 23 March 2024; accepted 14 April 2024. Date of publication 19 April 2024; date of current version 23 May 2024. This work was supported by the European Union (EU) Project HORIZON-RIA-LOLIPOP under Contract 101070441. The review of this letter was arranged by Editor R.-H. Horng. *(Corresponding author: Lis K. Nanver.)*

Lis K. Nanver, Vinayak V. Hassan, and Asma Attariabad are with the MESA+ Institute for Nanotechnology, University of Twente, 7522 NH Enschede, The Netherlands (e-mail: l.k.nanver@utwente.nl).

Nicholas Rosson and Chantal J. Arena are with Lawrence Semiconductor, Tempe, AZ 85282 USA.

Color versions of one or more figures in this letter are available at https://doi.org/10.1109/LED.2024.3391729.

Digital Object Identifier 10.1109/LED.2024.3391729

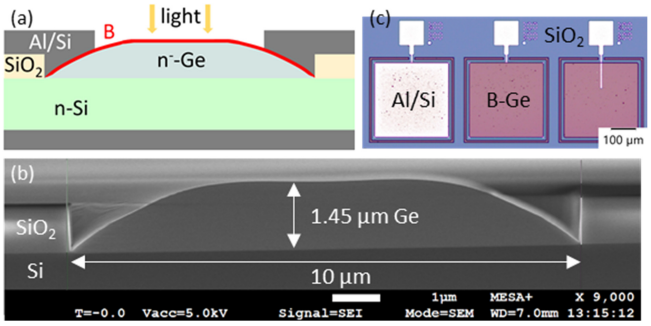

Fig. 1. Schematic diode cross section (a) and corresponding scanning electron microscopy image (b). (c) Optical microscopy images of diode contacting with (left to right) full, ring and finger metal coverage.

TABLE I
BORON DEPOSITION PARAMETERS AND PROPERTIES

Sample	Dep. Temp (°C)	Dep. Pres-sure (torr)	Thickness + roughness (nm)	ρ_c (kΩ-cm^{-2})	Etch rate (nm/min)	Ge doping 10^{15} cm^{-3}
B700AT	700	760	9.4+1.4	29±8	0.034	1.0
B700RP	700	20	10.8+2.2	1.2±0.2	0.083	3.0
B575AT	575	760	12.7+9.5	9.7±6.3	0.41	1.2
B575RP	575	20	11.0+1.4	4.9±2.7	0.34	1.02

Spectro- scopic ellipsometry (SE) was used to estimate the thickness of the B and Ge as-grown layers; results are given in Table I. The B-layer was modeled with two regions: the first region directly on the Ge containing a compact homogeneous B film and a surface region of incomplete (non-compact) B coverage commonly referred to as the roughness layer [17].

For comparison purposes, the 4 B-layer types were also de-posited on wafers with oxide windows to bare Si. Contacting was performed by lifting off 1-μm sputtered Al/Si(1%). As shown in Fig. 1, photodiodes with different Al coverage of the photosensitive area were available. As a last step, the samples were alloyed at 400°C to improve Al adhesion.

Optoelectronic measurements were performed at 25°C using an in-house setup built around a Karl Suss MicroTec PM300 wafer-prober, as described in detail in [18]. A Keithley 4200 parameter analyzer was used to measure *C-V* and *I-V* characteristics, the latter also while exposing the diodes to laser light from a 4-channel laser source, Thorlabs MCLS1, using fiber-coupled laser diodes. The available wavelengths were λ = 406 nm, 670 nm, 1310 nm, and 1550 nm. The fiber was connected to the lamp adapter of the probe station to focus the whole spot on the central region of the diodes. The optical power received by the diodes was measured using Thorlabs slide power sensors: the S120C (Si) for 400 - 1100 nm and S122C (Ge) for 700 - 1800 nm wavelengths.

III. ELECTRICAL MEASUREMENTS AND MATERIAL ANALYSIS

Examples of the *I-V* characteristics of the Ge diodes are shown in Fig. 2a and compared to PureB Si diodes. All Ge diodes, had an ideality factor n = 1 and close to the same forward current at 0.14 V. This is also the case independent

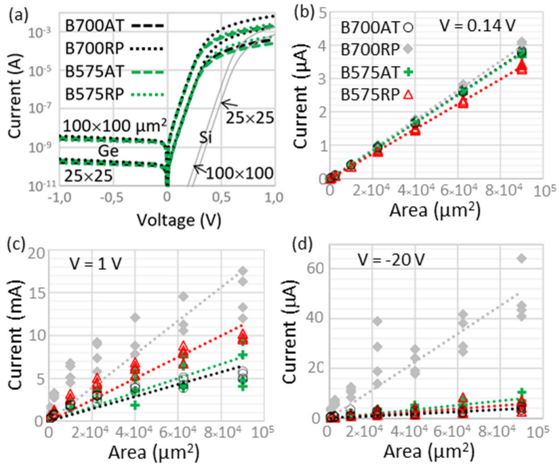

Fig. 2. (a) *I-V* characteristics of PureB Ge diodes with full Al-contacting compared to Si diodes. Area dependence of *I* at (b) 0.14 V forward, (c) 1 V forward, and (d) 20 V reverse voltage; with dotted trend lines.

of Al-coverage of the anode showing that the metal does not affect the critical B-Ge interface properties. At V = 0.14 V, I increases linearly with area (Fig. 2b), while at higher V it becomes attenuated by series resistance and differences between the devices are large (Fig. 2c). At high reverse V = 20 V, differences in I are also evident (Fig. 2d).

The series resistance through the B-layer was estimated from the diode *I-V* characteristics as well as transmission-line measurements on structures contacting the B-layer. The corre-sponding contact resistivity, ρ_c, is listed in Table I. The ρ_c is very high which is in agreement with the B resistivity values known from PureB Si research to be in the order of kΩ-cm [9]. In contrast, the sheet resistance along the B-Ge interface is in all cases ~ 3 kΩ/sq which is about 4 times lower than for similar Si devices, indicating the mobility advantage of Ge.

Earlier PureB Si studies have shown that the B-layer density increased with deposition temperature [19]. The high contact resistivity of the B700AT B-layer, suggests that this is also the case here. The etch rates in RT Al-etchant were measured and listed in Table I. The B-layers deposited on the Si-only samples did not etch at RT but required 45°C for B-removal [19]. Thus the B deposited on Ge was much more loosely bonded than on Si, but the 700°C B-layers did etch slower than the 575°C layers. The perfection of the substrate surface also plays a role [20]. Here the samples with high Ge defect densities clearly have less perfect B-layers.

From PureB Si studies we have seen that with B deposited at 450°C–700°C even 3-nm-thin layers formed a material barrier to Al, Au and Cu [12]. However, for deposition below 400°C the B-layers were very loosely bonded and pure Al metallization would penetrate weak spots, forming Schottky diodes to the Si and significantly increasing electron injection into the PureB anodes [21]. Such Schottky formation was prevented by applying Al/Si(1%), perhaps because Si precipitates, p-doped with Al, preferentially form on the Si surface. By using Al/Si(1%) for the present Ge experiments a Schottky-free B-Ge interface was maintained even for the most loosely bonded B-layers. However, the lowering of the contact

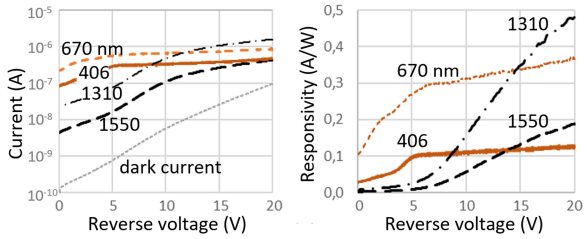

Fig. 3. Reverse current and responsivity of a B700AT photodiode with area 25 × 25 μm^2 and exposure to 4 different wavelengths.

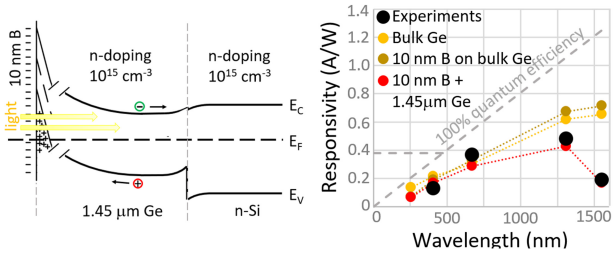

Fig. 4. Left: Bandgap diagram illustrating the barrier for electron injection into the n-Si substrate, and the strong band-bending at the Ge surface in the presence of a high concentration of fixed negative charge at the B-Ge interface. Right: The experimental responsivity of B700AT at 20 V reverse bias, compared to the theoretical responsivity calculated at 406, 670, 1310, and 1550 nm for 3 different combinations of B and Ge, joined by dotted lines.

resistance does show that Al was penetrating further into the less dense layers.

Doping profiles were extracted from *C-V* measurements and they are listed in Table I. The difference in doping levels between the samples can be caused by differences in the density of donor-type defects and/or memory effects during deposition.

For both the Ge and Si diodes, the hole injection is determined by the integral n-doping of the Si substrate. The decades higher saturation current of the Ge diodes is therefore dominated by electron injection into the anode, the Gummel number of which corresponds to an integral p-doping of 4×10^{14} cm^{-2}, very similar to that of PureB Si diodes [14].

IV. Optical Characterization

The optoelectrical *I-V* characteristics and responsivity are shown in Fig. 3 for a B700AT 25 × 25 μm^2 ring-contacted diode that displayed one of the lowest dark current levels. At 0 V the responsivity is low but increases with reverse biasing. The Ge should be depleted at about 0.8 V reverse bias which should help to increase the responsivity, particularly for the longer wavelengths. However, with the doping levels and bandgaps of the Ge and Si used in these experiments, a potential barrier at the Ge-Si interface, as illustrated in Fig. 4, will inhibit the collection of electrons at the Si cathode. This barrier can also be higher if acceptor-type defects are present at the Ge-Si interface. The barrier can be reduced by increasing the reverse voltage and the responsivity increases steadily when going up to 20 V, more so for the two long wavelengths that do not benefit from detection in the Si.

Similar results were found for the other samples but the responsivity values were consistently lower when dark currents were higher, indicating that the defects were also causing recombination of light-generated carriers. Most of the measured samples displayed responsivity within 80% of the B700AT values, but on sample B575RP the responsivity levels were reduced by as much as 50% with large spread. This sample was visually more defected than the other samples and also had a high B etch rate. Hence it is plausible that the Ge defects are the main cause of these reductions in responsivity.

In Fig. 4 the B700AT responsivity is compared to the "ideal" responsivity calculated using the optical parameters for Ge and Si from [22], [23], and [24]. The B parameters (Table II) were measured in house by SE on Si samples. The effect of Ge defects was omitted. The analysis shows that for the short wavelengths, the absorption in the B is the most limiting factor while for the long wavelengths the Ge thickness limits the detection. Variations in layer thickness/roughness will impact the experimental results but the trend and amounts of both theoretical and experimental values are very similar, indicating that sample B700AT has close to ideal responsivity.

TABLE II
Optical Constants for B-Layers

Wave-length (nm)	n	k	Absorption coefficient (cm^{-1})	Absorption length (nm)	Minimum anti-reflective coating on Ge (nm) [25]
406	3.509	0.817	252670	39.5773	28.93
670	3.319	0.303	56923.7	175.674	50.46
1310	3.198	0.099	9478.16	1055.06	102.4
1550	3.182	0.078	6314.57	1583.64	121.8

V. Conclusion

All the studied B-layer depositions resulted in the same low diode saturation current of 40 μA/cm^2 corresponding to an anode Gummel number equivalent to a high integral p-doping of 4×10^{14} cm^{-2}. In agreement with this the sheet resistance along the B-Ge p-type interface region, was a low 3 kΩ/sq. In contrast, the overall optoelectrical performance of PureB Ge (photo)diodes was to a large extent dependent on the quality of the Ge. Not only did the otherwise close to ideal responsivity decrease and dark currents increase with increasing Ge defect density but also the density of the B-layer was deteriorated. This allowed an increased penetration of Al into the B. The density of the B-layer was in all cases much lower than comparable layers on Si. This, and the dependence on Ge quality, will make the direct contacting of tunneling B-layers needed for low series resistance, such as routinely applied in PureB Si photodiodes, more challenging.

References

[1] J. Liu, "Monolithically integrated Ge-on-Si active photonics," *Photonics*, vol. 1, no. 3, pp. 162–197, Jul. 2014, doi: 10.3390/photonics1030162.

[2] K. Yamada, T. Tsuchizawa, H. Nishi, R. Kou, T. Hiraki, K. Takeda, H. Fukuda, Y. Ishikawa, K. Wada, and T. Yamamoto, "High-performance silicon photonics technology for telecommunications applications," *Sci. Technol. Adv. Mater.*, vol. 15, no. 2, Apr. 2014, Art. no. 024603, doi: 10.1088/1468-6996/15/2/024603.

[3] M. Bosi and G. Attolini, "Germanium: Epitaxy and its applications," *Prog. Crystal Growth Characterization Mater.*, vol. 56, nos. 3–4, pp. 146–174, Sep. 2010, doi: 10.1016/j.pcrysgrow.2010.09.002.

[4] M. F. B. Amin, T. Hizawa, J. A. Piedra-Lorenzana, T. Nakai, and Y. Ishikawa, "Reduced threading dislocation density in a Ge epitaxial film on a submicron-patterned Si substrate grown by chemical vapor deposition," *J. Electron. Mater.*, vol. 52, no. 8, pp. 5059–5065, Aug. 2023, doi: 10.1007/s11664-023-10302-3.

[5] V. A. Shah, A. Dobbie, M. Myronov, and D. R. Leadley, "Effect of layer thickness on structural quality of Ge epilayers grown directly on Si(001)," *Thin Solid Films*, vol. 519, no. 22, pp. 7911–7917, Sep. 2011, doi: 10.1016/j.tsf.2011.06.022.

[6] L. K. Nanver and T. Knezevic, "Optical detectors," in *Advances in Semiconductor Technologies: Selected Topics Beyond Conventional CMOS*, 1st ed., A. Chen, Ed. Hoboken, NJ, USA: Wiley, 2022, ch. 11, pp. 211–229, doi: 10.1002/9781119869610.

[7] Y. Ruan, C. Chen, S. Huang, W. Huang, S. Chen, C. Li, and J. Li, "Influence of implantation damages and intrinsic dislocations on phosphorus diffusion in Ge," *IEEE Trans. Electron Devices*, vol. 60, no. 11, pp. 3741–3745, Nov. 2013, doi: 10.1109/TED.2013.2280382.

[8] A. Chroneos and H. Bracht, "Diffusion of *n*-type dopants in germanium," *Appl. Phys. Rev.*, vol. 1, no. 1, Mar. 2014, Art. no. 011301, doi: 10.1063/1.4838215.

[9] L. K. Nanver, L. Qi, V. Mohammadi, K. R. M. Mok, W. B. de Boer, N. Golshani, A. Sammak, T. L. M. Scholtes, A. Gottwald, U. Kroth, and F. Scholze, "Robust UV/VUV/EUV PureB photodiode detector technology with high CMOS compatibility," *IEEE J. Sel. Topics Quantum Electron.*, vol. 20, no. 6, pp. 306–316, Nov. 2014, doi: 10.1109/JSTQE.2014.2319582.

[10] A. Sakic, G. van Veen, K. Kooijman, P. Vogelsang, T. L. M. Scholtes, W. B. de Boer, J. Derakhshandeh, W. H. A. Wien, S. Milosavljevic, and L. K. Nanver, "High-efficiency silicon photodiode detector for sub-keV electron microscopy," *IEEE Trans. Electron Devices*, vol. 59, no. 10, pp. 2707–2714, Oct. 2012, doi: 10.1109/TED.2012.2207960.

[11] L. Qi and L. K. Nanver, "Conductance along the interface formed by 400 °C pure boron deposition on silicon," *IEEE Electron Device Lett.*, vol. 36, no. 2, pp. 102–104, Feb. 2015, doi: 10.1109/LED.2014.2386296.

[12] S. D. Thammaiah, T. Knezevic, and L. K. Nanver, "Nanometer-thin pure boron CVD layers as material barrier to Au or Cu metallization of Si," *J. Mater. Sci., Mater. Electron.*, vol. 32, pp. 7123–7135, Mar. 2021, doi: 10.1007/s10854-021-05422-719.

[13] A. Sammak, L. Qi, W. B. de Boer, and L. K. Nanver, "Chemical vapor deposition of Ga dopants for fabricating ultrashallow p-n junctions at 400 °C," in *Proc. 10th IEEE Int. Conf. Solid-State Integr. Circuit Technol.*, Nov. 2010, pp. 969–971, doi: 10.1109/ICSICT.2010.5667503.

[14] L. K. Nanver, L. Qi, X. Liu, and T. Knežević, "Nanolayer boron-semiconductor interfaces and their device applications," *Solid-State Electron.*, vol. 186, Dec. 2021, Art. no. 108041, doi: 10.1016/j.sse.2021.108041.

[15] A. Sammak, M. Aminian, L. Qi, W. B. de Boer, E. Charbon, and L. K. Nanver, "A CMOS compatible Ge-on-Si APD operating in proportional and Geiger modes at infrared wavelengths," in *IEDM Tech. Dig.*, Washington, DC, USA, Dec. 2011, pp. 8.5.1–8.5.4, doi: 10.1109/IEDM.2011.6131515.

[16] T. Knežević, M. Krakers, and L. K. Nanver, "Broadband PureGaB Ge-on-Si photodiodes responsive in the ultraviolet to near-infrared range," *Proc. SPIE*, vol. 11276, Mar. 2020, Art. no. 112760I, doi: 10.1117/12.2546734.

[17] D. Lehmann, F. Seidel, and D. R. Zahn, "Thin films with high surface roughness: Thickness and dielectric function analysis using spectroscopic ellipsometry," *SpringerPlus*, vol. 3, no. 1, pp. 1–8, Dec. 2014, doi: 10.1186/2193-1801-3-82.

[18] M. Krakers, T. Knežević, and L. K. Nanver, "Optoelectrical operation stability of broadband PureGaB Ge-on-Si photodiodes with anomalous Al-mediated sidewall contacting," *J. Electron. Mater.*, vol. 50, no. 12, pp. 7026–7036, Dec. 2021, doi: 10.1007/s11664-021-09233-8.

[19] X. Liu, J. Italiano, R. Scott, and L. K. Nanver, "Silicon micromachining with nanometer-thin boron masking and membrane material," *Mater. Res. Exp.*, vol. 6, no. 11, Nov. 2019, Art. no. 116438, doi: 10.1088/2053-1591/ab4b03.

[20] L. K. Nanver, K. Lyon, X. Liu, J. Italiano, and J. Huffman, "Material reliability of low-temperature boron deposition for PureB silicon photodiode fabrication," *MRS Adv.*, vol. 3, nos. 57–58, pp. 3397–3402, Nov. 2018, doi: 10.1557/adv.2018.506.

[21] T. Kneževic, X. Liu, E. Hardeveld, T. Suligoj, and L. K. Nanver, "Limits on thinning of boron layers with/without metal contacting in PureB Si (photo)diodes," *IEEE Electron Device Lett.*, vol. 40, no. 6, pp. 858–861, Jun. 2019, doi: 10.1109/LED.2019.2910465.

[22] D. E. Aspnes and A. A. Studna, "Dielectric functions and optical parameters of Si, Ge, GaP, GaAs, GaSb, InP, InAs, and InSb from 1.5 to 6.0 eV," *Phys. Rev. B*, vol. 27, no. 2, pp. 985–1009, Jan. 1983, doi: 10.1103/physrevb.27.985.

[23] C. Schinke, P. C. Peest, J. Schmidt, R. Brendel, K. Bothe, M. R. Vogt, I. Kröger, S. Winter, A. Schirmacher, S. Lim, H. T. Nguyen, and D. MacDonald, "Uncertainty analysis for the coefficient of band-to-band absorption of crystalline silicon," *AIP Adv.*, vol. 5, no. 6, Jun. 2015, doi: 10.1063/1.4923379.

[24] T. N. Nunley, N. S. Fernando, N. Samarasingha, J. M. Moya, C. M. Nelson, A. A. Medina, and S. Zollner, "Optical constants of germanium and thermally grown germanium dioxide from 0.5 to 6.6 eV via a multisample ellipsometry investigation," *J. Vac. Sci. Technol. B, Nanotechnol. Microelectron., Mater., Process., Meas., Phenomena*, vol. 34, no. 6, Nov. 2016, doi: 10.1116/1.4963075.

[25] K. Nelaturu. *Thin-Film Optical Coating Calculator*. Accessed: Jan. 2024. [Online]. Available: https://www.omnicalculator.com/physics/thin-film-optics